

Spin-echo measurements on dilute ^{197}Au in iron and nickel

P. C. Riedi

Department of Physics, University of St. Andrews, St. Andrews, Fife, KY16 9SS, Scotland, United Kingdom

E. Hagn

Physik-Department, Technische Universität München, D-8046 Garching bei München, Federal Republic of Germany

(Received 27 March 1984)

Spin-echo measurements on ^{197}Au were performed on dilute alloys of Au (0.1 and 0.01 at.%) in Fe and Ni at 4.2 and 1.4 K. The magnetic hyperfine splitting frequencies $\nu_M = |g\mu_N B_{\text{hf}}/h|$ extrapolated to 0 K were determined to be $\nu_M(\text{AuFe}) = 93.207(10)$ MHz and $\nu_M(\text{AuNi}) = 21.59(3)$ MHz. For $\text{Au}(0.1 \text{ at.}\%)\text{Fe}$, the local-moment-induced electric quadrupole splitting could be resolved. The quadrupole splitting frequency $\nu_Q = e^2qQ/h$ was found to be $(-1.50(5))$ MHz. With the known quadrupole moment of ^{197}Au , $Q = +0.547(16)$ b, the electric field gradient of AuFe is deduced to be $(-0.113(6)) \times 10^{17}$ V/cm². With the known quadrupole splittings of ^{198}Au and ^{199}Au in Fe taken into account, the spectroscopic quadrupole moments of ^{198}Au and ^{199}Au are deduced to be $Q(^{198}\text{Au}; 2^-) = 0.76(4)$ b and $Q(^{199}\text{Au}; \frac{3}{2}^+) = 0.55(3)$ b. The experimental hyperfine anomalies between ^{197}Au , ^{198}Au , and ^{199}Au in Fe and Ni are discussed in the context of noncontact hyperfine fields.

I. INTRODUCTION

At the site of a substitutional impurity atom in dilute alloys of cubic, ferromagnetic Fe, fcc Co, or Ni, a small local-moment-induced electric field gradient (EFG) exists in addition to the large magnetic hyperfine field, which originates from the unquenched orbital momentum of the d electrons at the impurity site. Especially for $5d$ Ir in Fe and Ni this effect is relatively large; it was first detected by the spin-echo measurements by Aiga and Itoh¹ on ^{191}Ir and ^{193}Ir in Fe and Ni, who detected a splitting of the NMR resonance into three subresonances separated equidistantly (^{191}Ir and ^{193}Ir both have spin $\frac{3}{2}$). While these measurements were sensitive to signals from the domain walls, further double-resonance experiments on ^{191}Ir and ^{193}Ir in Fe and Ni showed a similar behavior of the signals originating from nuclei in domains.² Experiments performed on Ir in Fe single crystals² showed no dependence of the EFG on crystal directions. These findings were in accordance with the results of Mössbauer-effect measurements on ^{193}Ir in Fe,^{3,4} which mainly are sensitive to nuclei in domains. First nuclear magnetic resonance on oriented nuclei detected via nuclear radiation⁵ (NMR-ON) on radioactive ^{192}Ir ($j=4$) in Ni showed an asymmetric resonance structure, but the subresonances were not resolved because of the overly large inhomogeneous linewidth.⁶ Systematic NMR-ON studies on ^{192}Ir in Fe and Ni showed that the inhomogeneous linewidth could be reduced considerably by preparing extremely diluted alloys and by a careful annealing procedure. In this way the quadrupole subresonance structure of ^{192}Ir in Fe and Ni could be resolved well.⁷ In subsequent NMR-ON measurements on ^{194}Ir ($j=1$) in Fe and Ni the quadrupole splitting could also be resolved.⁸ The ratios of the quadrupole splittings of ^{192}Ir and ^{194}Ir in Fe and Ni, which resulted from NMR-ON measurements, which are

sensitive only to nuclei in domains, were in good agreement with the corresponding ratio of ^{193}Ir , derived from the spin-echo experiments sensitive to nuclei in domain walls. Thus quadrupole-interaction-resolved NMR and NMR-ON spectroscopy is a suitable interlink between stable and radioactive nuclei, for the determination of spectroscopic quadrupole moments of radioactive isotopes with resonance precision, as the quadrupole moments of stable isotopes can be measured with high precision via muonic x-ray spectroscopy.⁹ In addition, the local-moment-induced EFG in cubic metals is an interesting quantity by itself.

For Au in Fe and Ni the situation is similar to that of Ir, and EFG's of similar magnitude were expected. It turned out, however, that the inhomogeneous linewidths were too large compared to the subresonance separation. Thus it seemed to be impossible to resolve the quadrupole subresonance structure. For ^{198}Au and ^{199}Au in Fe, Callaghan *et al.*^{10,11} reported measurements of the quadrupole splitting using the technique of "single-passage" NMR on oriented nuclei. With this technique¹² it should, in principle, be possible to determine a quadrupole splitting which is small compared to the resonance linewidth. As the interpretation of single-passage NMR spectra depends on parameters, which cannot be determined experimentally, and for which "reasonable" assumptions must be made, the quadrupole splittings of $^{198}\text{AuFe}$ and $^{199}\text{AuFe}$ derived by Callaghan *et al.*^{10,11} contained uncertainties, even in their sign. For $^{199}\text{AuFe}$ Callaghan *et al.*¹¹ also reported the detection of the quadrupole splitting in a frequency-modulated-NMR-ON measurement. Recently, the subresonance structures of ^{199}Au and ^{198}Au in Fe were resolved directly^{13,14} by using extremely diluted alloys containing 0.1–0.01 at. % Au. Thus there was a realistic hope that the quadrupole subresonance structure of stable ^{197}Au in Fe could be resolved as well.

As the quadrupole moment of ^{197}Au is known from muonic x-ray measurements,¹⁵ $Q = +0.547(16)$ b, a NMR measurement on $^{197}\text{AuFe}$ could serve as an interlink to the determination of quadrupole moments of radioactive Au isotopes, which are interesting since Au lies in a transition region of nuclei between the well-deformed rare-earth nuclei and the spherical nuclei near ^{208}Pb .

In addition, a precise knowledge of the hyperfine splitting of dilute ^{197}Au in Fe and Ni was desirable in order to clarify the discrepancies on the hyperfine anomalies between ^{197}Au , ^{198}Au , and ^{199}Au reported recently.¹⁴ The experimental hyperfine anomalies in Fe and Ni, together with known hyperfine anomalies in a pure contact-interaction environment,¹⁶ yield information on the non-contact contribution to the hyperfine field, which is expected to be directly correlated with the local-moment-induced EFG.

Here we report spin-echo measurements on dilute ^{197}Au in Fe and Ni. Our measurements showed that spin-echo measurements are possible on extremely diluted alloys. The inhomogeneous linewidths could be reduced considerably, yielding hyperfine splittings with much improved accuracy.

II. EXPERIMENTAL DETAILS

Samples of $^{197}\text{AuFe}$ were prepared in the following way: ^{197}Au was melted with highly pure iron (purity >99.999%) in an electron-beam furnace, the ^{197}Au concentration being 0.1 at. %. In a further melting step the alloy was diluted with pure iron to a final concentration of 0.01 at. %. Foils with an area of 20×30 mm² and a thickness of ~ 1.5 μm were prepared by cold-rolling. The foils were annealed for ~ 3 h at $\sim 650^\circ\text{C}$ in vacuum ($\leq 10^{-6}$ Torr). Special care was taken in slowly cooling them down to room temperature, a process performed continuously in a time interval of ~ 4 h. $^{197}\text{AuNi}$ samples were prepared in similar manner. The foils were interleaved with mica foil, rolled into a cylinder, and inserted in a tuned circuit matched to the 50- Ω transmission line. At helium temperature Q was adjusted to 30 for AuFe and 60 for the AuNi sample. The higher Q value was necessary for AuNi, partly because of the inherent weakness of the ^{197}Au NMR due to the lower value of the Au hyperfine field in this system, and partly because of experimental difficulties due to the interference from the 10 MHz clock of the signal averager.

Spin echoes were excited and observed using a phase-coherent NMR spectrometer.¹⁷ The rf power was sufficiently low for only domain-wall-enhanced NMR to be observed. At each frequency the echo was integrated at (unknown) phase ϕ with respect to the reference and then at $\phi + \pi/2$. The intensity was then found from $S = (S_\phi^2 + S_{\phi+\pi/2}^2)^{1/2}$. Detailed measurements were made near 93.2 MHz for AuFe and 21.6 MHz for AuNi to establish the line center. The accuracy of the measurements of the line centers depended on the linewidth and signal-to-thermal-noise ratio for the AuFe sample, but was lowered for the AuNi sample by interference from the clock of the signal averager.

The ^{197}Au signal from the Au(0.1 at. %)Fe sample was

sufficiently strong for the quadrupole satellite lines to be observed. In addition, the in-phase echo at the center of the main line was not a simple bell-shaped curve, but showed structure with a period Δt such that $1/\Delta t = 0.74(3)$ MHz, in agreement with the frequency difference between the main and satellite lines.

III. RESULTS AND DISCUSSION

Figure 1 shows the NMR spectrum of the $^{197}\text{Au}(0.1$ at. %)Fe sample measured at 4.2 K. As ^{197}Au has a ground-state spin of $\frac{3}{2}$, three equidistant resonances are expected for a collinear magnetic-dipole-plus-electric-quadrupole interaction, and they are located at ν_M , $\nu_M \pm \Delta\nu_Q$, where

$$\nu_M = |g\mu_N B_{\text{hf}}/h|, \quad \nu_Q = e^2qQ/h, \quad (1)$$

$$\Delta\nu_Q = 3\nu_Q/[2j(2j-1)].$$

Here, ν_M and ν_Q are the usually quoted magnetic and electric hyperfine splitting frequencies; g and Q are the nuclear g factor and the nuclear spectroscopic quadrupole moment, respectively; B_{hf} and eq are the magnetic hyperfine field and the electric field gradient, respectively.

The solid line in Fig. 1 is the result of a least-squares fit performed with the assumption of three Lorentzian lines separated equidistantly by $\Delta\nu_Q$. The linewidth of the central line and the linewidths of the two satellite lines were taken as independent parameters. The fit yields

$$\nu_M = 93.198(10) \text{ MHz}, \quad |\nu_Q| = 1.50(5) \text{ MHz}.$$

For the $^{197}\text{Au}(0.01$ at. %)Fe sample the observed signal was very weak even though the measurements were performed at 1.4 K. Thus the quadrupole splitting could not be detected. As the center of the main line coincided well with the result obtained for the 0.1 at. % sample, no further attempt was made to resolve the quadrupole interaction. For the $^{197}\text{Au}(0.1$ at. %)Ni sample the observed signals were also weak. The main line could be resolved

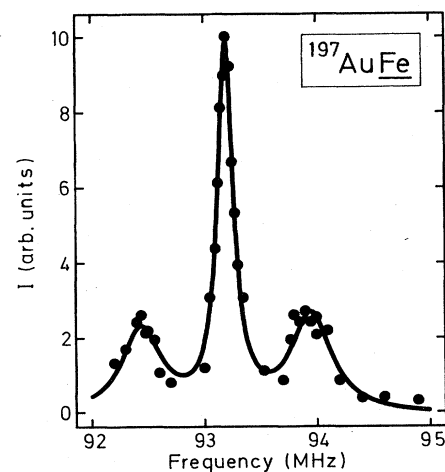


FIG. 1. Quadrupole-interaction-resolved NMR signal from $^{197}\text{Au}(0.1$ at. %)Fe measured at 4.2 K. The full width at half maximum is 0.17(1) MHz for the central line and 0.42(9) MHz for the satellites.

well, but the quadrupole satellites could not be detected. In Table I the results of the present work are compiled, together with the result on a Au(1 at. %)Fe powder sample.¹⁸ As expected, the linewidths obtained with the 0.1- and 0.01-at. % foils of the present work are considerably smaller than that of the 1 at. % powder sample. A more striking result is the fact that the resonance centers are different, which means that a concentration dependence of the magnetic hyperfine interaction of ¹⁹⁷AuFe exists, even in the concentration range 0.1–1 at. %.

The temperature dependence of the hyperfine field of ¹⁹⁷Au in iron, measured in a sample containing 1 at. % Au, is much stronger than that of the magnetization of iron.^{18,19} Assuming that the same temperature dependence holds for the 0.1- and 0.01-at. % Au samples, the correction to 0 K is 9 kHz for 4.2 K and 2 kHz for 1.4 K. The temperature dependence of the hyperfine field of Au in Ni has not been reported, but the correction to 0 K from 1.4 K must be less than 1 kHz in this case since the hyperfine field in Ni is only 0.23 times as large as in iron.

Ratios of hyperfine splittings of different Au isotopes in Fe and Ni are listed in Table II. The ratio for ¹⁹⁷Au of the present work, $R = 4.317(6)$, is in good agreement with the ratios of the other isotopes. This is an essential result, as the present data result from the hyperfine interactions in domain walls, while the data for all other isotopes represent the hyperfine interaction originating from nuclei in domains. This shows that there is no fundamental difference between the hyperfine interaction of nuclei in domain walls or domains. It is the dependence of the hyperfine interaction on the impurity concentration which simulates discrepancies between NMR and NMR-ON if the NMR data originate from measurements on systems with relatively high impurity concentrations. It should be noted that all the ratios of Table II are well described by a Gaussian distribution with an average value $R = 4.323(2)$. This is a further indication that the NMR-ON data on ¹⁹⁶AuNi and ¹⁹⁸AuNi of Ref. 23 are incorrect.

The magnetic splittings of ¹⁹⁷Au, ¹⁹⁸Au, and ¹⁹⁹Au in Fe, and ¹⁹⁷Au and ¹⁹⁸Au in Ni, which are listed in Table II, are now used to derive the hyperfine anomalies between these isotopes in Fe and Ni. These hyperfine anomalies, together with the known values in an environment with a pure contact interaction, allow the determination of the noncontact contributions to the hyperfine field of Au in Fe and Ni.

The hyperfine anomaly ${}^1\Delta^2$ between two nuclear states of isotopes "1" and "2" is defined as

$$a_1/a_2 = (g_1/g_2)(1 + {}^1\Delta^2), \quad (2)$$

where $a_{1,2}$ are the magnetic hyperfine splitting frequencies and $g_{1,2}$ are the respective g factors. The hyperfine anomaly is due to the fact that a contact hyperfine field may vary considerably over the nuclear volume for high- Z nuclei, which has the consequence that the spin and orbital parts of the nuclear magnetic moments "see" different "effective" hyperfine fields. The total effective hyperfine field thus depends strongly on the particular nuclear wave function. In Table III we have listed the experimental ratios of hyperfine splittings and g factors. The "contact" hyperfine anomalies are ${}^{197}\Delta_c^{198} = 0.0853(8)$, ${}^{197}\Delta_c^{199} = 0.037(2)$, and ${}^{198}\Delta_c^{199} = -0.045(3)$.²⁴ It is obvious that the ratios ${}^1\Delta_{Fe}^2/{}^1\Delta_c^2$ and ${}^1\Delta_{Ni}^2/{}^1\Delta_c^2$ represent the fractional contribution of the contact fields to the hyperfine fields in Fe and Ni. This ratio, which is given by

$${}^1R_{Fe,Ni}^2 = \left[\frac{(a_1/a_2)_{Fe,Ni}}{(a_1/a_2)_c} (1 + {}^1\Delta_c^2) - 1 \right] / {}^1\Delta_c^2, \quad (3)$$

should be independent of the pair 1,2 used for the calculation. The results for ${}^{197}R_{Fe}^{198}$, ${}^{197}R_{Fe}^{199}$, and ${}^{198}R_{Fe}^{199}$ are 1.135(3), 1.141(11), and 1.118(10), respectively, in good agreement with an average value 1.135(3). All discrepancies reported in Ref. 14 concerning this ratio are now removed. For Ni the ratio is $R_{Ni} = 1.145(21)$; this proves that the fractional contribution of the noncontact hyperfine field to the total hyperfine field is, within the experimental uncertainty, equal for Fe and Ni. Taking $B_{hf}(AuFe) = -1145(17)$ kG and $B_{hf}(AuNi) = -264.4(3.9)$ kG, the noncontact hyperfine fields for Au in Fe and Ni are deduced to be +155(5) and +38(6) kG, respectively.

The electric hyperfine splitting frequencies of ¹⁹⁷Au, ¹⁹⁸Au, and ¹⁹⁹Au in Fe are listed in Table IV, together with Mössbauer-effect data on ¹⁹⁷Au in Cd and Zn,²⁵ and nuclear orientation data on ¹⁹⁸Au and ¹⁹⁹Au in Cd and Zn.²⁶ In order to facilitate the comparison, we added the ratios $R = \nu_Q/\nu_Q(^{197}Au)$ for Fe, and $R_{Cd,Zn}$, which represent ratios of nuclear spectroscopic quadrupole moments, and which thus should be independent of the host lattices and the type of measurement. It is obvious, how-

TABLE I. Magnetic hyperfine splitting frequencies for ¹⁹⁷Au in Fe and Ni extrapolated to 0 K.

System	Concentration (at. %)	Form	T (K)	Main line (MHz)	Full width at half maximum (MHz)
¹⁹⁷ AuFe	1	powder	4.2	93.52 ^{a,b}	1.1
¹⁹⁷ AuFe	0.1	foil	4.2	93.207(10) ^b	0.17
¹⁹⁷ AuFe	0.01	foil	1.4	93.201(15) ^c	0.05 ^d
¹⁹⁷ AuNi	0.1	foil	1.4	21.59(3) ^e	0.16

^aReference 18; quadrupole splitting obscured by width of main line.

^bCorrection from 4.2 to 0 K according to Ref. 19: 9 kHz.

^cCorrection from 1.4 to 0 K according to Ref. 19: 2 kHz.

^dVery weak signal. Full width at half maximum is estimated from width of echo.

^eNo temperature correction applied.

TABLE II. Experimental magnetic hyperfine splittings and ratios of hyperfine splittings of Au isotopes in Fe and Ni.

Isotope	ν_{Fe} (MHz)	ν_{Ni} (MHz)	$\nu_{\text{Fe}}/\nu_{\text{Ni}}$
$^{195\text{m}}\text{Au}$	980.38(11) ^a	226.58(12) ^a	4.327(3)
^{197}Au	93.207(10) ^b	21.59(3) ^b	4.317(6)
$^{197\text{m}}\text{Au}$	949.2(6) ^c	219.72(4) ^c	4.320(3)
^{198}Au	259.48(3) ^d	60.06(5) ^e	4.320(4)
$^{198\text{m}}\text{Au}$	425.5(3) ^c	98.40(1) ^c	4.324(3)
^{199}Au	166.69(4) ^f		
Average			4.323(2)

^aReference 20.^bThis work.^cReference 21.^dReference 14.^eReference 22.^fReference 13.

ever, that the ratios from the “integral” Mössbauer-effect and nuclear-orientation measurements are inconsistent with the resonance data of the present work and of Ref. 13 and 14. This means that one of the two sets of data is incorrect.

In the present NMR experiment the quadrupole interaction frequency for $^{197}\text{AuFe}$ was derived from resonance spectra, where the quadrupole splitting was resolved uniquely. The ratios of the integrated intensity of the main line to the satellite lines are 1.7(5) and 1.4(4), which are considered to be in agreement with the theoretical value of 1.33. The subresonance structure is similar to the structure of ^{191}Ir and ^{193}Ir in Fe and Ni,^{1,2} for which the quadrupolar origin of the splitting was proven.²

In the NMR-ON experiments on $^{199}\text{AuFe}$ (Ref. 13) and $^{198}\text{AuFe}$ (Ref. 14), the quadrupole subresonance structure was also resolved. In addition, the quadrupolar origin of the subresonance structure was proven for $^{198}\text{AuFe}$. It has been shown in Ref. 14 that the quadrupole subresonance structure of the NMR-ON resonances is different for $\theta=0^\circ$ and 90° , where θ is the angle of observation of the radiation with respect to the orientation axis, and that the 0° and 90° structures depend strongly on the β -decay matrix elements of ^{198}Au . The β -decay matrix elements derived from the measured resonance spectra were in good agreement with data known experimentally from “conventional” nuclear-orientation measurements, which were considered as further independent proof of the quadrupolar origin of the subresonance structure. Furthermore, negative amplitudes were observed for the subresonance transitions corresponding to the energetically highest sublevels for $^{199}\text{AuFe}$ and $^{198}\text{AuFe}$, which is further proof for the quadrupolar origin of the subresonance structure,

which is discussed in detail in Refs. 13 and 14. In Ref. 2 it was shown that the quadrupole splitting of ^{191}Ir and ^{193}Ir in Fe and Ni is not different for nuclei in domain walls and nuclei in domains. This is additionally supported by Mössbauer-effect measurements on ^{193}Ir (Refs. 3 and 4) and NMR-ON measurements on ^{192}Ir and ^{194}Ir (Refs. 7 and 8). Thus there is no simple explanation that the resonance data on ^{197}Au , ^{198}Au , and ^{199}Au could have been misinterpreted.

The quadrupole interaction frequencies of ^{198}Au and ^{199}Au in Cd and Zn originate from (simultaneous) nuclear-orientation measurements at temperatures down to ~ 6 mK.²⁶ For this purpose, ^{198}Au and ^{199}Au were mass-separator-implanted into single crystals of Cd and Zn. Keeping in mind that typical mass-separator-implantation depths are ~ 500 Å, one can easily imagine that the surface quality of the single crystals plays an essential role, if the absolute magnitudes of the quadrupole splittings are to be determined. Moreover, the lattice location of the implanted impurity nuclei has to be known. In principle, the lattice location can be investigated with channeling techniques, which, in addition to nuclear orientation, has been done only in a few cases up to now. Depending on the type of impurity-host combination, it cannot be anticipated *a priori* that all implanted nuclei are substituted onto regular lattice sites. The electric field gradient acting on impurity nuclei on substitutional sites is, in general, completely different from the EFG on interstitial sites, the latter depending, in addition, on the type of interstitial site. Those effects should be known for a correct interpretation of integral hyperfine-interaction measurements on mass-separator-implanted samples. Ratios of quadrupole splittings and thus ratios of quadrupole moments are less affected by such effects, if they are deduced from simultaneous measurements on different isotopes, as the uncertainties in the lattice location and the reduction of the hyperfine interaction due to crystal imperfections cancel out in first approximation.²⁷

The Mössbauer-effect measurements on ^{197}Au were performed with sources of $^{197\text{m}}\text{Hg}$ and ^{197}Hg prepared also by mass-separator implantation. This means that all problems mentioned before also apply to these measurements. There is, however, a decisive additional difference: Krien *et al.*²⁸ studied the implantation behavior of Hg and Au in Zn. They found that of Au atoms implanted into Zn, a fraction greater than 85% occupied substitutional lattice sites, in agreement with solubility predictions.²⁹ For Hg, however, a very low solid solubility in Zn is known.³⁰ Channeling data indicated nearly complete random site occupation of Hg in Zn.²⁸ No unique quadrupole interaction was found with the time-dependent perturbed-angular-correlation technique. For Hg in Cd no single-

TABLE III. Ratios of hyperfine splittings and g factors of Au isotopes. Ratios for Fe and Ni are calculated with the data of Table II.

Isotopes	g_1/g_2	$(a_1/a_2)_c$	$(a_1/a_2)_{\text{Fe}}$	$(a_1/a_2)_{\text{Ni}}$
^{197}Au , ^{198}Au	0.327 48(22) ^a	0.355 426 363(7) ^a	0.359 21(6)	0.359 47(58)
^{197}Au , ^{199}Au	0.536 8(14) ^a	0.556 369 102(15) ^a	0.559 16(15)	
^{198}Au , ^{199}Au	1.639 2(44) ^a	1.565 356 876(52) ^a	1.556 66(40)	

^aReference 24.

TABLE IV. Electric hyperfine splitting frequencies of Au isotopes and ratios $R = \nu_Q / \nu_Q(^{197}\text{Au})$.

Isotope	$\nu_Q^{(\text{Fe})}$ (MHz)	R_{Fe}	$\nu_Q^{(\text{Cd})}$ (MHz)	$\nu_Q^{(\text{Zn})}$ (MHz)	$R_{\text{Cd,Zn}}$
^{197}Au	(-)1.50(5) ^a	1.0	+155(6) ^b	+200(30) ^b	1.0
^{198}Au	-2.09(4) ^c	1.39(5)	+130(4) ^d	+162(3) ^d	0.85(4)
^{199}Au	-1.52(2) ^e	1.01(4)	+107(3) ^d	+127(2) ^d	0.68(3)

^aThis work.^bReference 25.^cReference 14.^dReference 26.^eReference 13.

crystal implantation data exist; the implantation behavior into polycrystalline foils³¹ does not allow unique conclusions to be drawn in this context. Perscheid and Haas²⁵ completely neglected the difference of the implantation behavior of Au and Hg. Moreover, their Mössbauer spectra are not resolved and the quadrupole interaction was deduced from the line broadening and the (small) shift of the effective resonance centers for the resonance absorption parallel and perpendicular to the c axis. From the data given in Ref. 25 it is difficult to believe that all necessary corrections, such as the finite absorber thickness, angular dependence of the Lamb-Mössbauer factor, etc. (which strongly affect the value of the deduced quadrupole splitting), have been determined with sufficient accuracy. It should be noted that a small fraction of implanted nuclei on interstitial lattice sites may introduce a larger effect onto the deduced "substitutional" EFG. For example, the EFG of Hg in Be is, for interstitial sites, a factor of ~ 13 larger than the EFG on substitutional sites.³²

Thus we conclude that the ratios of quadrupole splittings and the quadrupole moments [$Q(^{198}\text{Au})=0.46(2)$ b and $Q(^{199}\text{Au})=0.37(1)$ b] given by Perscheid and Haas²⁵ are incorrect.

Taking the quadrupole splittings in Fe given in Table IV and the quadrupole moment of ^{197}Au , $Q=0.547(16)$ b,¹⁵ we derive the quadrupole moments of ^{198}Au and ^{199}Au ,

$$Q(^{198}\text{Au})=0.76(4) \text{ b}, \quad Q(^{199}\text{Au})=0.55(3) \text{ b}.$$

The present experiment does not allow the derivation of the sign of the EFG or, thus, the sign of the quadrupole moments. The systematics of EFG's in noncubic metals^{33,34} suggests that the EFG's of impurities in Zn and Cd are positive. From the NO measurements²⁶ a positive sign of the quadrupole moments of ^{198}Au and ^{199}Au is thus inferred.

The local-moment-induced EFG of ^{79}Au in Fe is deduced to be

$$eq(\text{AuFe})=(-)0.113(6)\times 10^{17} \text{ V/cm}^2,$$

which is smaller by a factor of 2.3 than the corresponding EFG of neighboring ^{77}Ir , $eq(\text{IrFe})=-0.260(5)\times 10^{17} \text{ V/cm}^2$ [Ref. 7, recalculated with the quadrupole moment $Q(^{193}\text{Ir})=0.815(9)$ b (Ref. 9)]. The noncontact hyperfine fields, which also originate from the unquenched orbital momenta of the $5d$ electrons, for Au and Ir in Fe, are +155(5) and +155(90) kG,³⁵ respectively. There have been several attempts to calculate these EFG's,³⁶⁻³⁸ but the quantitative results have not been satisfactory. To our knowledge, local-moment-induced EFG's have been observed up to now only for Ir in Fe and Ni,^{1,2} Au in Fe and Co in Co,³⁹⁻⁴¹ Ni in Ni,⁴² Co in Fe,⁴³ and Fe in Fe.⁴⁴ As small EFG's have also been observed in the pure systems FeFe, CoCo, and NiNi—pure systems having the advantage of a small inhomogeneous linewidth—local-moment-induced EFG's may exist in general. Our experiments have shown that spin-echo measurements can be performed on extremely diluted alloys, for which the inhomogeneous linewidths can be reduced considerably by appropriate sample preparation. Thus it should be possible to resolve the quadrupole splitting for other impurities in Fe and Ni as well.

Note added in proof. A distribution of hyperfine fields consistent with Fig. 1, but without clearly resolved satellite lines, has been observed in a 0.2-at. % Au sample by J. I. Budnick and T. J. Burch (unpublished) (private communication from Budnick).

ACKNOWLEDGEMENTS

We want to thank Dr. P. Maier-Komor, E. Kellner, and J. Hesol for the sample preparation. Discussions with Dr. E. Zech are gratefully acknowledged. The work of one of us (E.H.) was supported by the Bundesministerium für Forschung und Technologie, Bonn, Germany; the work of P.C.R., by the Science and Engineering Research Council.

¹M. Aiga and J. Itoh, J. Phys. Soc. Jpn. 31, 1844 (1971).²M. Aiga and J. Itoh, J. Phys. Soc. Jpn. 37, 967 (1974).³F. Wagner and W. Potzel, in *Hyperfine Interactions in Excited Nuclei*, edited by G. Goldring and R. Kalish (Gordon and Breach, New York, 1971), Vol. 2, p. 681.⁴D. Salomon and D. A. Shirley, Phys. Rev. B 9, 29 (1974).⁵E. Matthias and R. J. Holliday, Phys. Rev. Lett. 17, 897 (1966).⁶P. D. Johnston and N. J. Stone, J. Phys. C 5, L303 (1972).⁷E. Hagn, K. Leuthold, E. Zech, and H. Ernst, Phys. Lett. 85B, 321 (1979); Z. Phys. A 295, 385 (1980).⁸E. Hagn, H. Kleebauer, M. Zahn, and E. Zech, Z. Phys. A 306, 73 (1982).

- ⁹Y. Tanaka, R. M. Steffen, E. B. Shera, W. Reuter, M. V. Hoehn, and J. D. Zumbro, *Phys. Rev. Lett.* **51**, 1633 (1983).
- ¹⁰P. T. Callaghan, P. D. Johnston, W. M. Lattimer, and N. J. Stone, *Phys. Rev. B* **12**, 3526 (1975).
- ¹¹P. T. Callaghan, W. M. Lattimer, P. D. Johnston, and N. J. Stone, *Hyperfine Interact.* **2**, 288 (1976).
- ¹²P. T. Callaghan, P. D. Johnston, W. M. Lattimer, and N. J. Stone, *J. Phys. C* **7**, 3161 (1974).
- ¹³E. Hagn and E. Zech, *Z. Phys. A* **307**, 159 (1982).
- ¹⁴E. Hagn and E. Zech, *Phys. Rev. B* **29**, 1148 (1984).
- ¹⁵R. J. Powers, P. Martin, G. H. Miller, R. E. Welsh, and D. A. Jenkins, *Nucl. Phys. A* **230**, 413 (1974).
- ¹⁶G. J. Perlow, in *Hyperfine Interactions in Excited Nuclei*, Ref. 3, Vol. 2, p. 651.
- ¹⁷G. D. Webber and P. C. Riedi, *J. Phys. E* **14**, 1159 (1981).
- ¹⁸G. D. Webber and P. C. Riedi, *J. Phys. F* **11**, L29 (1981).
- ¹⁹P. C. Riedi and G. D. Webber, *J. Phys. F* **11**, 1669 (1981).
- ²⁰E. Hagn, E. Zech, and G. Eska, *Phys. Rev. C* **24**, 631 (1981).
- ²¹E. Hagn and E. Zech, *Nucl. Phys. A* **417**, 88 (1984).
- ²²E. Hagn and E. Zech, *Hyperfine Interact.* **15-16**, 93 (1983).
- ²³F. Bacon, G. Kaindl, H.-E. Mahnke, and D. A. Shirley, *Phys. Rev. C* **7**, 1654 (1973).
- ²⁴P. A. Vanden Bout, V. J. Ehlers, W. A. Nierenberg, and H. A. Shugart, *Phys. Rev.* **158**, 1078 (1967).
- ²⁵B. Perscheid and H. Haas, *Hyperfine Interact.* **15-16**, 227 (1983).
- ²⁶P. Herzog, K. Freitag, H. Hildebrand, M. Reuschenbach, and H. Walitzki, *Z. Phys. A* **314**, 215 (1983).
- ²⁷E. Hagn, S. Jönsson, C. Trautmann, and E. Zech, *Hyperfine Interact.* **15-16**, 245 (1983).
- ²⁸K. Krien, F. Reuschenbach, J. C. Soares, R. Vianden, R. Trzcinski, K. Freitag, M. Hage-Ali, and P. Siffert, *Hyperfine Interact.* **7**, 413 (1980).
- ²⁹J. R. Chelikowsky, *Phys. Rev. B* **19**, 686 (1979).
- ³⁰R. P. Elliot, *Constitution of Binary Alloys* (McGraw-Hill, New York, 1965), Suppl. 1.
- ³¹K. Krien, J. C. Soares, K. Freitag, R. Vianden, and A. G. Biliboni, *Hyperfine Interact.* **1**, 217 (1975).
- ³²K. Krien, F. Reuschenbach, J. C. Soares, P. Herzog, H.-R. Folle, B. Perscheid, R. Trzcinski, and K. Freitag, *Hyperfine Interact.* **7**, 401 (1980).
- ³³P. Raghavan, E. N. Kaufmann, R. S. Raghavan, E. J. Ansaldo, and R. A. Naumann, *Phys. Rev. B* **13**, 2835 (1976).
- ³⁴H. Ernst, E. Hagn, E. Zech, and G. Eska, *Phys. Rev. B* **19**, 4460 (1979).
- ³⁵F. E. Wagner, *Hyperfine Interact.* **13**, 149 (1983).
- ³⁶C. Demangeat, *J. Phys. F* **4**, L64 (1974); **5**, 169 (1975).
- ³⁷G. A. Gehring and H. C. W. L. Williams, *J. Phys. F* **4**, 291 (1974).
- ³⁸V. Zevin, D. Fekete, and N. Kaplan, *Phys. Rev. B* **17**, 355 (1978).
- ³⁹P. C. Riedi and R. G. Scurlock, *Phys. Lett.* **24A**, 42 (1967).
- ⁴⁰D. Fekete, H. Boasson, A. Grayevski, V. Zevin, and N. Kaplan, *Phys. Rev. B* **17**, 347 (1978).
- ⁴¹E. Hagn and E. Zech, *Phys. Rev. B* **25**, 1529 (1982).
- ⁴²H. Enokiya and M. Kawakami, *J. Phys. Soc. Jpn.* **50**, 2221 (1981).
- ⁴³P. T. Callaghan, W. M. Lattimer, P. D. Johnston, and N. J. Stone, *Hyperfine Interact.* **2**, 291 (1976).
- ⁴⁴J. Spijkerman, J. C. Travis, D. N. Pipkorn, and C. E. Violet, *Phys. Rev. Lett.* **26**, 323 (1971).